

## Precision Measurement of the $\Omega^-$ Magnetic Moment

N. B. Wallace, P. M. Border, D. P. Ciampa, G. Guglielmo,\* K. J. Heller, and D. M. Woods  
*School of Physics and Astronomy, University of Minnesota, Minneapolis, Minnesota 55455*

K. A. Johns

*Department of Physics, University of Arizona, Tucson, Arizona 85721*

Y. T. Gao† and M. J. Longo

*Department of Physics, University of Michigan, Ann Arbor, Michigan 48109*

R. Rameika

*Fermi National Accelerator Laboratory, Batavia, Illinois 60510*

(Received 26 October 1994)

Using a sample of  $2.35 \times 10^5$  polarized  $\Omega^- \rightarrow \Lambda K^-$  decays, we have measured the  $\Omega^-$  magnetic moment to be  $\mu_{\Omega^-} = (-2.024 \pm 0.056)\mu_N$ .

PACS numbers: 13.40.Em, 13.30.Eg, 14.20.Jn

The structure of baryons can be probed at long range by measuring their magnetic moments. For example, the ratio of the proton and neutron magnetic moments offered early support for the quark model of baryons. There now exist precise measurements of the magnetic moments of the  $\Lambda$  [1],  $\Sigma^+$  [2,3],  $\Sigma^-$  [4,5],  $\Xi^0$  [6,7], and  $\Xi^-$  [8–10], as well as the  $\Xi^+$  [11] and  $\Sigma^-$  [3] antihyperons. Together with the very precisely measured proton and neutron moments, these measurements have been used to test models of baryon structure [12]. Such models have only been successful to the 10% level, perhaps because these baryons have a more complex structure than expected. A measurement of the  $\Omega^-$  magnetic moment is of interest due to its simple valence quark structure (three strange quarks with their spins aligned). Because of this symmetry, and because the  $\Omega^-$  has no light valence quarks ( $u$  or  $d$ ), this system is expected to have smaller relativistic and orbital angular momentum corrections than may be present in the octet baryons [13]. The only previous measurement of the  $\Omega^-$  magnetic moment [14], to a precision of 10%, could not clearly differentiate between models of baryon structure.

The traditional spin-precession technique for measuring hyperon magnetic moments uses a beam of polarized hyperons produced from proton interactions [1,15]. The hyperon spin is then precessed in a magnetic field and the final spin direction is measured from the asymmetry of the distribution of the hyperon decay products. Unlike the spin  $\frac{1}{2}$  hyperons,  $\Omega^-$ 's produced by protons are unpolarized [16]. In this experiment polarized  $\Omega^-$ 's were produced by using two different techniques: the spin transfer technique from a polarized neutral beam (PNB), which was used in the previous  $\Omega^-$  magnetic moment measurement [14], and a new technique that used an unpolarized neutral beam (UNB) [17]. In both cases a neutral beam containing  $\Lambda$  and  $\Xi^0$  hyperons, as well as  $\gamma$ 's, neutrons,

and  $K^0$ 's, was produced by an 800 GeV/c proton beam in the inclusive reaction  $p + \text{Be} \rightarrow (\text{neutral particle}) + X$ . In the unpolarized neutral beam mode, the protons struck an upstream target at 0 mrad. The resulting particles passed through a collimator embedded in a sweeping magnet with a field integral of 10.9 Tm. This neutral beam was then targeted at vertical production angles of  $\pm 1.8$  mrad on a second Be target to produce  $\Omega^-$ 's primarily by the reaction  $(\Lambda, \Xi^0) + \text{Be} \rightarrow \Omega^- + X$ . The polarized neutral beam was produced by targeting the proton beam at vertical targeting angles of  $\pm 1.8$  mrad, producing polarized  $\Xi^0$  and  $\Lambda$  [18,19]. Since the sweeping magnet field was perpendicular to the production plane, the spins of the neutral particles were not precessed as they passed through the channel. The  $\Omega^-$ 's were then produced by targeting the polarized neutral beam at 0 mrad. Table I shows the average polarizations for each of these modes. The  $\Omega^-$  yield per incident proton for unpolarized neutral beam production was roughly 3 times that for polarized neutral beam production.

The  $\Omega^-$  production target (Be,  $5.14 \times 5.28 \times 147 \text{ mm}^3$ ) was located 55 cm upstream from the spin-precession-momentum-selection magnet. The magnet was 7.315 m long with a field in the  $-\hat{y}$  direction. The magnet was fitted with a curved brass and tungsten

TABLE I. The sample sizes and average polarizations measured for the three  $\Omega^-$  samples used in this analysis. The initial polarization is in the  $\pm \hat{x}$  direction in a right-handed coordinate system defined by the  $\Omega^-$  momentum direction ( $\hat{z}$ ) and the vertical ( $\hat{y}$ ).

Production method	Precession field integral (T m)	Sample size $10^4$ events	$P_{\Omega^-}$
UNB	$-24.36 \pm 0.26$	16.7	$0.044 \pm 0.008$
UNB	$-17.48 \pm 0.17$	5.02	$0.036 \pm 0.015$
PNB	$-24.36 \pm 0.26$	1.83	$-0.069 \pm 0.023$

channel [20], with a total bend of 18.7 mrad in the  $x$ - $z$  plane and a defining aperture of  $5.08 \times 5.08$  mm. The curved channel selected negatively charged particles with a momentum range between 300 and 550 GeV/ $c$  when the magnet was operating at a field of 3.33 T. The field integral was measured to about 1% using a Hall probe [14] and checked by measuring the  $\Xi^-$  magnetic moment.

The parent  $\Omega^-$  and its charged daughters for the decay  $\Omega^- \rightarrow \Lambda K^-$  and  $\Lambda \rightarrow p \pi^-$  were detected using a spectrometer consisting of eight planes of silicon microstrip detectors (SSD's) with 100  $\mu$ m pitch, 12 multiwire proportional chambers (MWPCs) with 1 and 2 mm wire spacing, and an analyzing magnet consisting of two dipole magnets which gave a deflection of 1.45 GeV/ $c$  to the daughter  $p$ ,  $\pi^-$ , and  $K^-$  [21]. Signals from scintillation counters and wire chambers were used to form a trigger that required at least one positively charged and one negatively charged track in the spectrometer.

This simple trigger produced a data sample which contained 3.4%  $\Xi^-$  and 0.035%  $\Omega^-$  with a spectrometer live time of 70%. The approximately  $1.35 \times 10^9$  triggers were processed by a multipass off-line reconstruction program which fitted the three-track, two-vertex topology with an overall efficiency of 97% [17,20]. The events selected were required to fit the topology of the parent/daughter hyperon decay with the parent hyperon pointing back to within 8 mm of the center of the target in  $x$  and to within 9 mm in  $y$ .  $\Omega^-$  candidates were also required to have a  $\Lambda K^-$  invariant mass between 1657 and 1687 MeV/ $c$ . The  $\Xi^- \rightarrow \Lambda \pi^-$  decays reconstructed under the  $\Lambda K^-$  hypothesis which satisfy that mass criterion occupy a small range of decay angles in the  $\Omega^-$  rest frame [22]. All events in this range of decay angles were removed from the data sample, which according to simulation studies reduced the  $\Xi^-$  background to 0.6% of the final  $\Omega^-$  sample. The predominant remaining background,  $\Omega^- \rightarrow \Xi^0 \pi^-$  decays, determined to be about 2.4% of the final  $\Omega^-$  sample based on the measured branching ratio [23] and the detector resolution. The  $\Lambda K^-$  invariant mass is in Fig. 1 together with the expected distribution of  $\Omega^- \rightarrow \Lambda K^-$  events in our apparatus. The shape of the tails for these simulated events was based on the measured resolution of the  $\Xi^- \rightarrow \Lambda \pi^-$  decays in the apparatus. The level of the background from that distribution is less than 3%.

Assuming  $\gamma_{\Omega^-} = +1$ , the vector polarization of the  $\Omega^-$ ,  $\mathbf{P}_{\Omega^-}$ , is related to the daughter  $\Lambda$  polarization,  $\mathbf{P}_{\Lambda}$ , by  $\mathbf{P}_{\Omega^-} = \mathbf{P}_{\Lambda}$  [22]. The  $\Lambda$  polarization was determined by measuring the decay asymmetry of the proton in the  $\Lambda$  rest frame [18]. This measured asymmetry was corrected for acceptance by a hybrid Monte Carlo analysis [24]. The resulting proton distributions were then fitted to a linear function in  $\cos\theta$  for each component of the asymmetry.

For a negatively charged hyperon  $H$  with spin  $J$  (in units of  $\hbar$ ) passing through a precession field perpendicular to the initial polarization, the precession angle relative to its

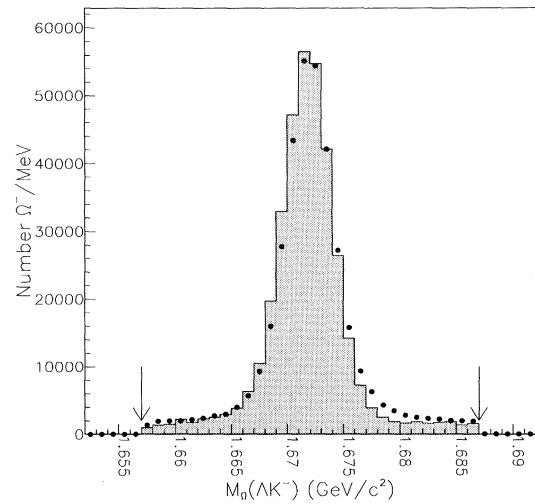


FIG. 1. The  $\Lambda K^-$  invariant mass. The solid histogram is the mass distribution for reconstructed Monte Carlo  $\Omega^-$  events. This histogram has been corrected for resolution using a comparison between the  $\Xi^-$  data and  $\Xi^-$  Monte Carlo mass distributions. The solid dots show the  $\Omega^-$  mass distribution for the entire data sample used for this measurement. The final mass selection criteria are indicated by the arrows. The difference between the tails of the distributions was used to determine the background to the  $\Omega^-$  sample.

momentum direction is given by

$$\Phi = \frac{e}{\beta m_H c} \left( \frac{m_H \mu_H}{2J m_p \mu_N} + 1 \right) \int B dl, \quad (1)$$

where  $\Phi$  is the precession angle in radians,  $e$  is the magnitude of the electron charge,  $\beta = v/c$ ,  $m_p$  is the mass of the proton,  $\mu_N$  is the nuclear magneton,  $m_H$  and  $\mu_H$  are the hyperon's mass and magnetic moment, and  $\int B dl$  is the precession field integral in Tm. Because parity is conserved in strong interactions, the initial polarization direction must be perpendicular to the production plane. In this case the measured polarization components are given by  $P_x = P_0 \cos\Phi$  and  $P_z = P_0 \sin\Phi$ , where  $\hat{z}$  is parallel to the  $\Omega^-$  momentum,  $\hat{y}$  is the vertical,  $\hat{x} = \hat{y} \times \hat{z}$ , and  $P_0$  is the initial hyperon polarization at the target. The precession angle is determined from the measured components of the polarization by  $\Phi = \arctan(P_z/P_x) + n\pi$  where  $n$  is an integer. The  $x$  and  $z$  components of the polarization, shown in Fig. 2, were significantly different from zero, while the  $y$  component for each sample was consistent with zero. Table II gives the precession angles and magnetic moments for the three samples for this experiment as well as the two samples from the previous experiment [14].

Using the three data samples of this experiment we found  $\mu_{\Omega^-}$  by minimizing

$$\chi^2 = \sum_{ij} \left( \frac{P_{x_{ij}} - P_{0_{ij}} \cos\Phi_j}{\sigma_{x_{ij}}} \right)^2 + \left( \frac{P_{z_{ij}} - P_{0_{ij}} \sin\Phi_j}{\sigma_{z_{ij}}} \right)^2, \quad (2)$$

TABLE II. The precession angles and magnetic moments measured for the three samples used in this analysis and the two samples from the previous measurement of  $\mu_{\Omega^-}$ .

Neutral beam type	Precession field integral (T m)	$\Phi$ (radians)	$\mu_{\Omega^-}$ (nuclear magnetons)
UNB	$-24.36 \pm 0.26$	$0.88 \pm 0.17$	$-2.023 \pm 0.065$
UNB	$-17.48 \pm 0.17$	$0.65 \pm 0.43$	$-2.03 \pm 0.23$
PNB	$-24.36 \pm 0.26$	$0.88 \pm 0.32$	$-2.02 \pm 0.12$
PNB [14]	$-19.53 \pm 0.19$	$0.58 \pm 0.42$	$-1.96 \pm 0.20$
PNB [14]	$-14.77 \pm 0.14$	$0.34 \pm 0.46$	$-1.90 \pm 0.29$

with  $\Phi_j$  given by Eq. (1).  $P_{0ij}$  is the initial polarization which depends on the production method.  $P_{xij}$  and  $P_{zij}$  are the measured  $x$  and  $z$  polarization components, and  $\sigma_{xij}^2$  and  $\sigma_{zij}^2$  include uncertainties from  $P_{xij}$  and  $P_{zij}$ . The subscript  $i$  indicates the production method, and the two precession field values are represented by the sum over  $j$ . The observed polarization at the target depends on the field integral, since the momentum spectrum of the particles entering the spectrometer changes with the field value. Minimizing the  $\chi^2$  defined in Eq. (2) gave  $\mu_{\Omega^-} = (-2.024 \pm 0.056)\mu_N$  with a  $\chi^2$  of  $1 \times 10^{-3}$  for two degrees of freedom. The uncertainty of the combined result is obtained by varying  $\mu_{\Omega^-}$  until the  $\chi^2$  defined in Eq. (2) increases by 1. The uncertainty obtained by this method agrees with expected statistical uncertainty from combining the three measurements.

The systematic uncertainties of this measurement were studied as a function of  $\Omega^-$  momentum (Fig. 3), decay vertex position, and the various selection criteria (such as the mass cut) used. The measured value of  $\mu_{\Omega^-}$  did not vary within statistical uncertainty as a function of any of these variables. The polarization of a sample produced

by a unpolarized neutral beam at 0.0 mrad was measured to be  $P_{0\text{mrad}} = (0.029 \pm 0.025)$ , consistent with zero as expected, since there is no clearly defined production plane. Another internal check is provided by comparing the precession angles of the unpolarized neutral beam and polarized neutral beam data samples. Even though the initial polarizations of these samples are in opposite directions (Fig. 2), their precession angles with the same precession field are the same (Table II). The stability of the result with various levels of  $\Xi^- \rightarrow \Lambda\pi^-$  and  $\Omega^- \rightarrow \Xi^0\pi^-$  backgrounds was studied both with Monte Carlo simulation and by varying the selection criteria on the data sample. The magnetic moment proved to be stable with background levels up to 3 times higher than those occurring in the final sample [21]. As a further check the  $\Xi^-$  magnetic moment was measured for the  $1.52 \times 10^6$  polarized  $\Xi^- \rightarrow \Lambda\pi^-$  events from the polarized neutral beam data using the same method as for the  $\Omega^-$  events. These events were recorded simultaneously with the  $\Omega^-$  events. This measurement gave  $\mu_{\Xi^-} = (-0.6478 \pm 0.0032)\mu_N$ , in agreement with previous measurements [10,23]. Unlike the  $\Omega^-$  events,  $\Xi^-$  events from the

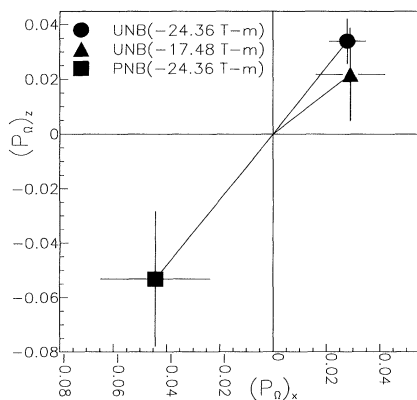


FIG. 2. The measured  $\hat{x}$  and  $\hat{z}$  polarization components for the three data samples used in this analysis. It should be noted that the initial polarization of the polarized neutral beam (PNB) sample is in the  $-\hat{x}$  direction, while the unpolarized neutral beam (UNB) production initial polarization is in the  $+\hat{x}$  direction. The angle between the lines and the horizontal axis is the precession angle.

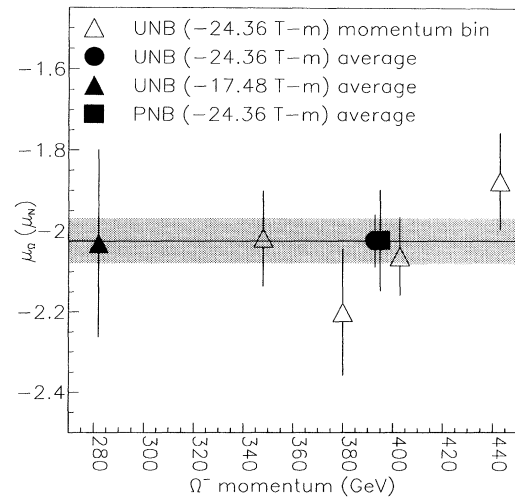


FIG. 3.  $\mu_{\Omega^-}$  vs  $\Omega^-$  momentum. The result of the constrained fit is shown by the line; the uncertainty of the constrained fit solution is shown by the shaded area.

unpolarized neutral beam were not polarized so their magnetic moment could not be measured.

The  $\Omega^-$  magnetic moments were measured independently for the three different conditions of this experiment and those of the previous measurement agree to within their measurement uncertainties. A linear fit for  $\Phi$  as a function of the precession field, constrained to include  $\Phi = 0$  for zero field, was used to remove the ambiguity of the precession angle due to rotations by an additional  $n\pi$ . The best fit for the points shown in Fig. 4 was for  $n = 0$  with a  $\chi^2 = 0.3$  for four degrees of freedom; the next best fit had  $\chi^2 = 10$  for  $n = 1$ .

Using the spin precession technique on polarized samples of  $\Omega^-$  produced by both polarized and unpolarized neutral beams, we have measured the magnetic moment of the  $\Omega^-$  to be  $\mu_{\Omega^-} = (-2.024 \pm 0.056)\mu_N$  with no evidence for any systematic error at the level of the statistical uncertainty. This agrees with the previous measurement of  $\mu_{\Omega^-} = (-1.94 \pm 0.17 \pm 0.14)\mu_N$ . Combining our result with the previous measurement gives a world average of  $\mu_{\Omega^-} = (-2.019 \pm 0.054)\mu_N$ , including the systematic uncertainty of the previous measurement. The line shown in Fig. 4 corresponds to this value of the magnetic moment. This measurement disagrees with the static quark

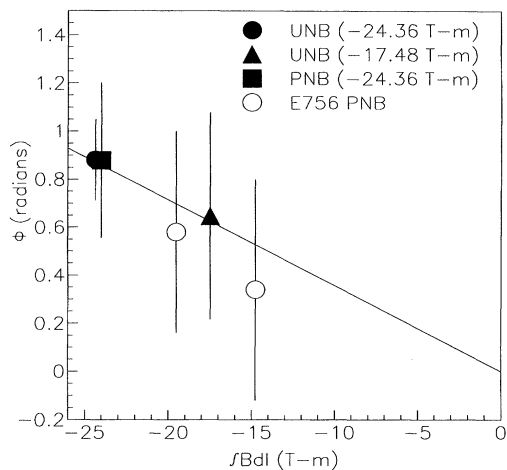


FIG. 4. The precession angle  $\Phi$  vs the field integral  $\int Bdl$ , including the E800 data samples and the previous measurements from Fermilab E756. The uncertainties shown are statistical only. The line for the world average value  $\mu_{\Omega^-}(-2.019 \pm 0.054)\mu_N$  is shown. The line fit has been constrained to pass through  $\Phi = 0$  for  $\int Bdl = 0$ .

model value of  $-1.84\mu_N$  at the  $3\sigma$  level and all other models known to the authors which successfully predict other magnetic moments. It is hoped that this measurement will provide a stringent test for future models of baryon structure.

This work was supported by the U.S. Department of Energy and the National Science Foundation. We would like to thank G. Allan, A. Ayala-Mercado, E. Berman, V. DeCarlo, D. Fein, M. Groblewski-Higgins, J. Jallian-Marian, E. James, R. McGriff, L. Morris, A. Nguyen, T. Tynan, and the staff of Fermi National Laboratory.

\*Present address: University of Oklahoma, Norman, OK 73069.

†Present address: University of Lanzhou, Lanzhou, China.

- [1] L. Schachinger *et al.*, Phys. Rev. Lett. **41**, 1348 (1978).
- [2] C. Wilkinson *et al.*, Phys. Rev. Lett. **58**, 855 (1987).
- [3] A. Morelos *et al.*, Phys. Rev. Lett. **71**, 3417 (1993).
- [4] Y. W. Wah *et al.*, Phys. Rev. Lett. **55**, 2551 (1985).
- [5] G. Zapalac *et al.*, Phys. Rev. Lett. **57**, 1526 (1986).
- [6] G. Bunce *et al.*, Phys. Lett. **86B**, 386 (1979).
- [7] P. T. Cox *et al.*, Phys. Rev. Lett. **46**, 877 (1981).
- [8] R. Rameika *et al.*, Phys. Rev. Lett. **52**, 581 (1984).
- [9] L. H. Trost *et al.*, Phys. Rev. D **46**, 1703 (1989).
- [10] J. Duryea *et al.*, Phys. Rev. Lett. **68**, 768 (1992).
- [11] P. M. Ho *et al.*, Phys. Rev. Lett. **65**, 1713 (1990).
- [12] K. Heller, in *Proceedings of the Seventh Lake Louise Winter Institute on Symmetry, Spin and the Standard Model*, edited by B. A. Campbell *et al.* (World Scientific, Singapore, 1992), p. 47, and the references contained therein.
- [13] H. J. Lipkin, Nucl. Phys. **B241**, 477 (1984).
- [14] H. T. Diehl *et al.*, Phys. Rev. Lett. **67**, 804 (1991).
- [15] K. Heller, J. Phys. **46**, 121 (1985), and references contained therein.
- [16] K. B. Luk *et al.*, Phys. Rev. Lett. **70**, 900 (1993).
- [17] D. M. Woods, Ph.D. thesis, University of Minnesota, 1995.
- [18] G. Bunce *et al.*, Phys. Rev. Lett. **36**, 1113 (1976).
- [19] P. T. Cox *et al.*, Phys. Rev. Lett. **51**, 2025 (1983).
- [20] G. M. Guglielmo, Ph.D. thesis, University of Minnesota, 1994.
- [21] N. B. Wallace, Ph.D. thesis, University of Minnesota, 1995.
- [22] K. B. Luk *et al.*, Phys. Rev. D **38**, 19 (1988).
- [23] Particle Data Group, Phys. Rev. D **50**, 1771 (1994).
- [24] G. Bunce, Nucl. Instrum. Methods **172**, 553 (1980).